

Studies of low-energy K- hadronic interactions with light nuclei by AMADEUS



Jagiellonian University in Krakow

Magdalena Skurzok*

On the behalf of the AMADEUS collaboration



Istituto Nazionale di Fisica Nucleare



The 18th International Conference on
Strangeness in Quark Matter (SQM 2019)
10-15 June 2019, Bari (Italy)

*magdalena.skurzok@lnf.infn.it

Plan

1. Motivation and scientific case
2. AMADEUS @ DAΦNE
3. Analysis results
4. Conclusions & perspectives

Motivation and Scientific Case

The investigation of the **in-medium modification of the $\bar{K}N$ interaction** is of **fundamental** for the low-energy QCD in the non perturbative regime.

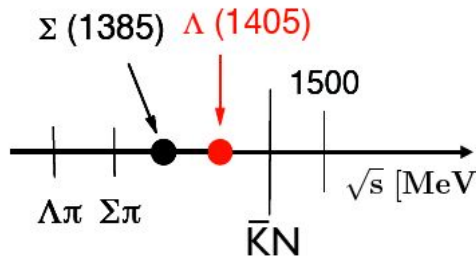
Chiral perturbation theory (ChPT): effective field theory where mesons and baryons represent the effective degrees of freedom instead of the fundamental quark and gluon fields.

$$\mathcal{L}_{eff} = \mathcal{L}_{mesons}(\Phi) + \mathcal{L}_B(\Phi, \Psi_B)$$

- The chiral symmetry is **spontaneously broken** \rightarrow the existence of massless and spinless Nambu-Goldstone bosons which are identified with the pions. Explicitly broken by q masses.
- **Very successful** in describing the πN , $\pi\pi$ and NN interactions in the low-energy regime and is considered as the theory of the low-energy strong interaction **in the SU(2) flavour sector**.

The extension of the theory to the sector with the quarks turns out to be more problematic since it is not directly applicable to the $\bar{K}N$ channel.

The χ PT is not applicable to the $\bar{K}N$ channel due to the emerging of the $\Lambda(1405)$ and the $\Sigma(1385)$ resonances just below the $\bar{K}N$ mass threshold



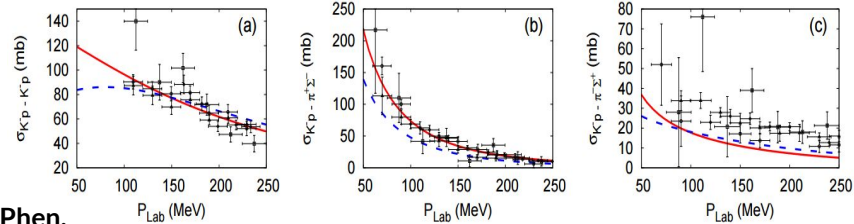
$\Lambda(1405)$ $I=0$ $J^P = \frac{1}{2}^-$
 $M = (1405.1^{+1.3}_{-1.0})$ MeV $\Gamma = (50.5 \pm 2.0)$ MeV
 decay modes: $\Sigma\pi$ ($I=0$) 100%

$\Sigma(1385)$ $I=1$ $J^P = 3/2^+$
 decay modes: $\Lambda\pi$ ($I=1$) (87.0 ± 1.5) %
 $\Sigma\pi$ ($I=1$) (11.7 ± 1.5) %

Possible solutions:

- Non-perturbative Coupled Channels approach: Chiral Unitary SU(3) Dynamics
- Phenomenological $\bar{K}N$ and NN potentials

The parameters of the models are constrained by the existing scattering data

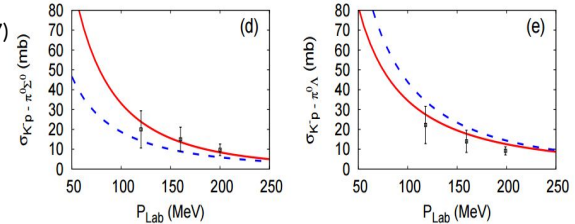


--- Phen.

Y. Ikeda and T. Sato, Phys. Rev. C76, 035203 (2007)

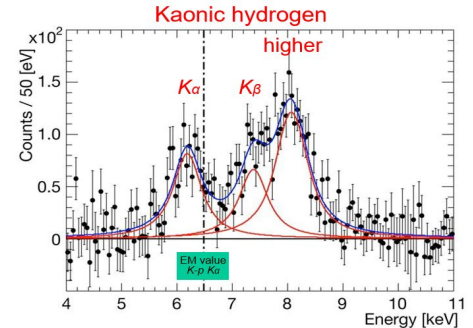
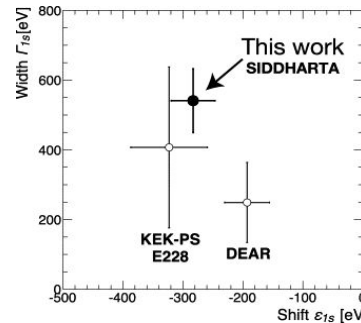
— Chiral

S. Ohnishi, Y. Ikeda, T. Hyodo, W. Weise, Phys.Rev. C93 (2016) no.2, 025207

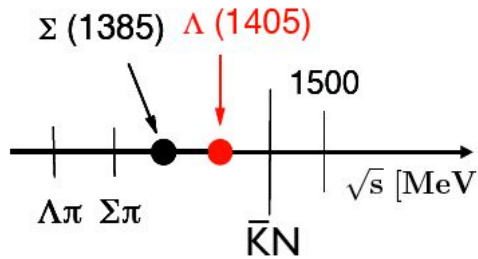


and by the SIDDHARTA measurement of K_α transition in Kaonic hydrogen at threshold

M. Bazzi et al., 2011. (SIDDHARTA Coll.), Phys. Lett. B704, 113



The χ PT is not applicable to the $\bar{K}N$ channel due to the emerging of the $\Lambda(1405)$ and the $\Sigma(1385)$ resonances just below the $\bar{K}N$ mass threshold



$\Lambda(1405)$ $I=0$ $J^P = \frac{1}{2}^-$

$M = (1405.1^{+1.3}_{-1.0})$ MeV $\Gamma = (50.5 \pm 2.0)$ MeV

decay modes: $\Sigma\pi$ ($I=0$) 100%

$\Sigma(1385)$ $I=1$ $J^P = 3/2^+$

decay modes: $\Lambda\pi$ ($I=1$) $(87.0 \pm 1.5)\%$

$\Sigma\pi$ ($I=1$) $(11.7 \pm 1.5)\%$

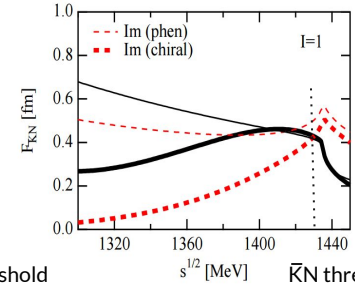
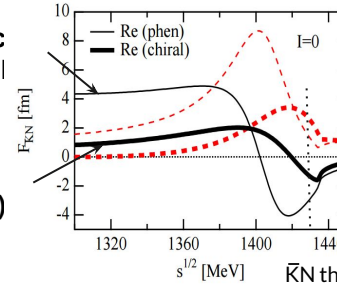
Possible solutions:

- **Non-perturbative Coupled Channels approach: Chiral Unitary SU(3) Dynamics**
- **Phenomenological $\bar{K}N$ and NN potentials**

...but... large differences in the subthreshold extrapolations!
Significantly weaker attraction in chiral SU(3) models than in phenomenological potential models.

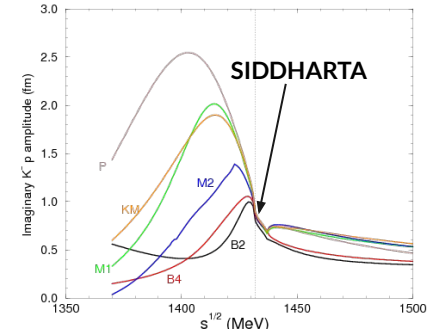
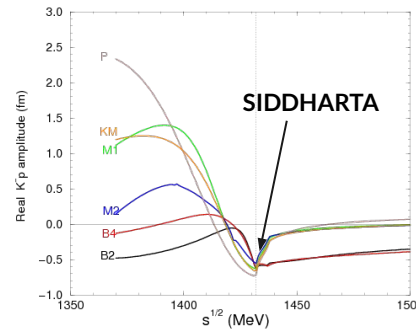
Re	Im	
—	- - -	Phen. [Y. Akaishi, T. Yamazaki, Phys. Rev. C65, 044005 (2002)]
—	- - -	Chiral [Y. Ikeda, T. Hyodo, W. Weise, Phys. Lett. B706, 63 (2011)]

Phenomenologic potential model



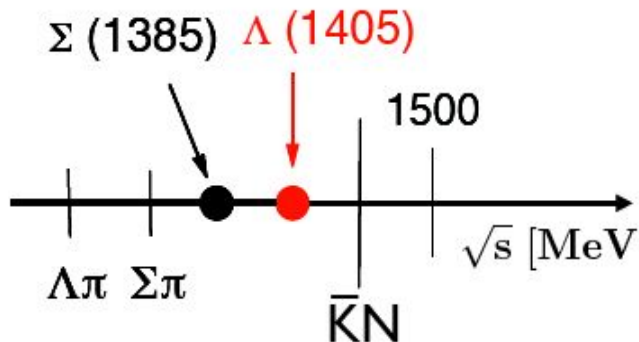
Chiral SU(3) dynamics

New experimental constraints!!!



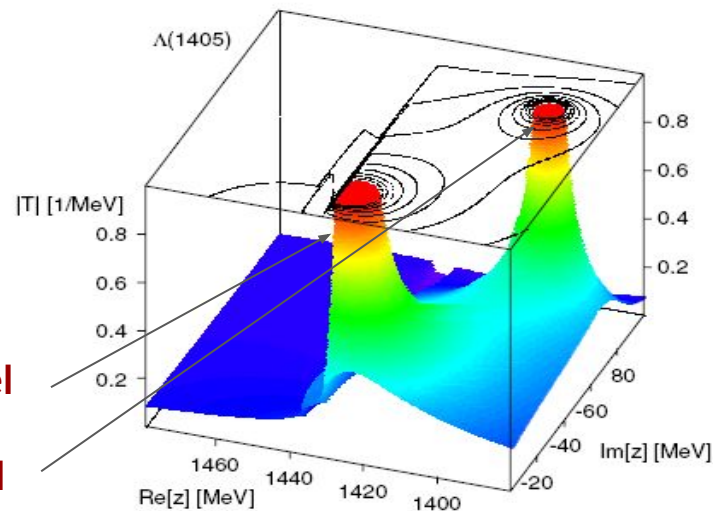
E. Friedman, A. Gal, Nucl. Phys. A959, 66 (2017)

The controversial nature of the $\Lambda(1405)$

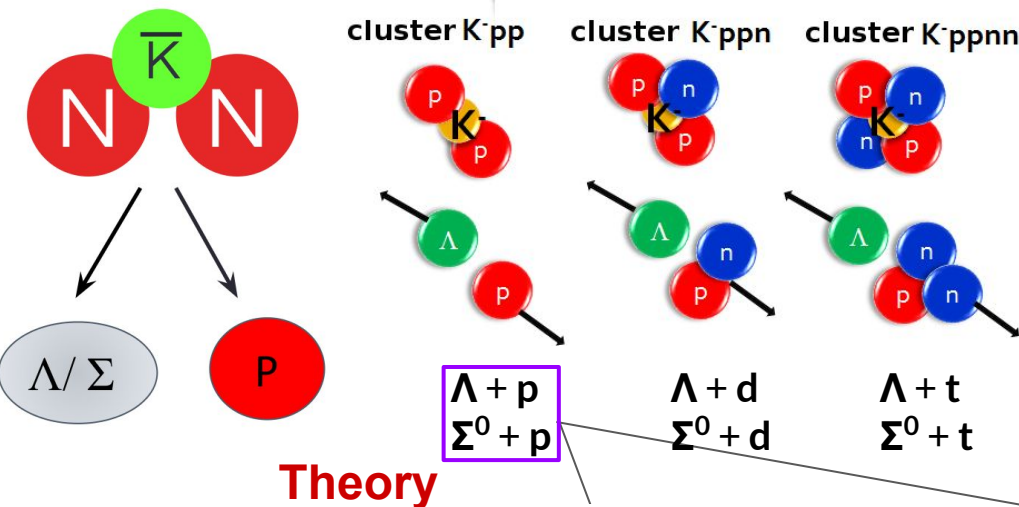


The $\Lambda(1405)$ state does not fit with the simple three quarks model (uds) and it is commonly accepted that it is, at least partially, a $\bar{K}N$ bound state.

- **Chiral SU(3) coupled channel dynamics:** the state is given by the superpositions of two poles of the $\bar{K}N$ scattering amplitude.
 $M = 1425 \text{ MeV} \rightarrow$ mainly coupled to the $\bar{K}N$ channel
 $M = 1380 \text{ MeV} \rightarrow$ mainly coupled to the $\Sigma\pi$ channel
- **Phenomenological potentials models:** the $\Lambda(1405)$ is a pure $\bar{K}N$ bound state with mass $M=1405 \text{ MeV}$, binding energy $BE = 27 \text{ MeV}$ and width $\Gamma=50 \text{ MeV}$.



Possible existence of kaonic bound states



Wycech (1986) - Akaishi & Yamazaki (2002)



Predicted in the $\bar{K}N$ interaction in the $I=0$ channel due to the strong interaction

Essential impact on the EoS of Neutron Stars
gravitational waves signal emitted by binary system of Neutron Stars

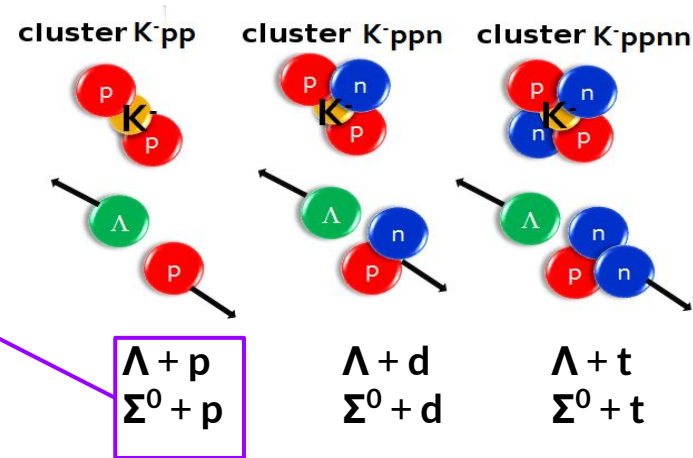
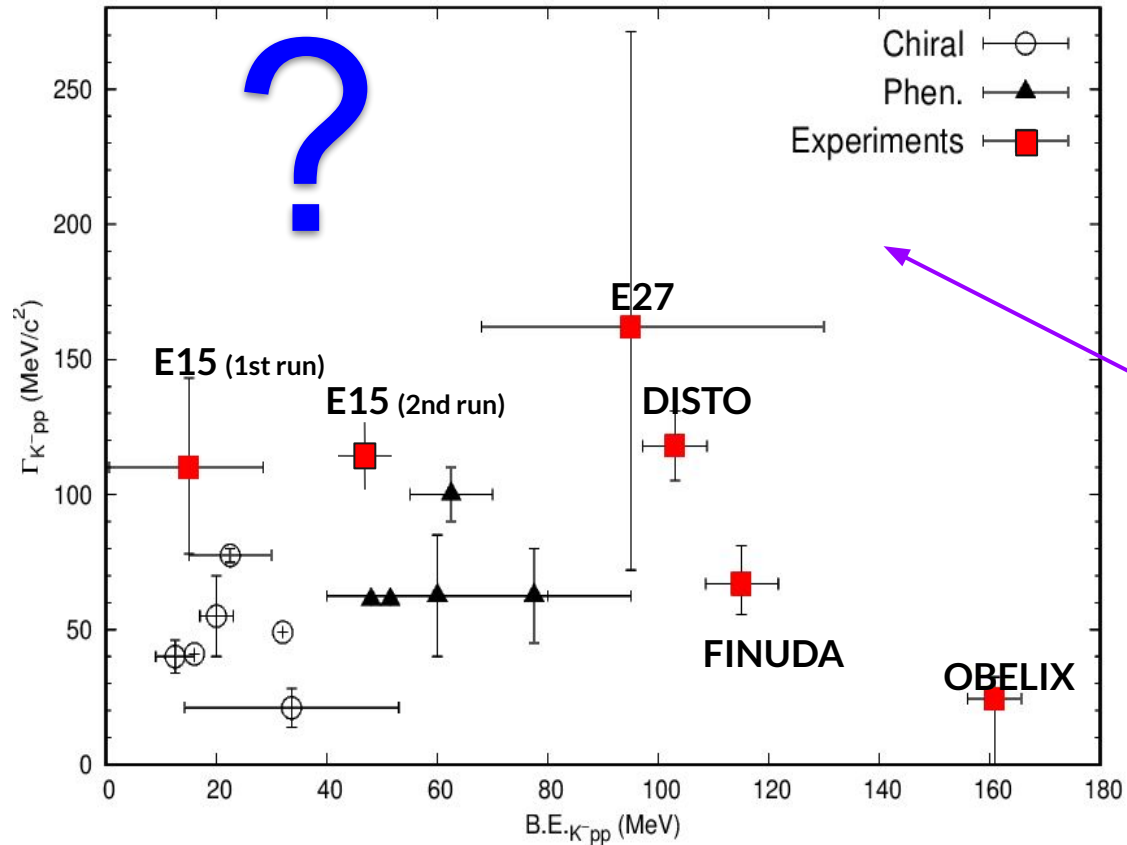
Theory

Experiments

Chiral models	BE [MeV]	Γ [MeV]	Reference
Dote, Hyodo, Weise	17 - 23	40 - 70	Phys. Rev. C 79 (2009) 014003
Barnea, Gal, Liverts	16	41	Phys. Lett. B 712 (2012) 132
Ikeda, Kamano, Sato	9 - 16	34 - 46	Prog. Theor. Phys. (2010) 124 (3)
Bicudo	14.2 - 53	13.8 - 28.3	Phys. Rev. D 76 (2007) 031502
Bayar, Oset	15 - 30	75 - 80	Nucl. Phys. A 914 (2013) 349
Dote, Inoue, Myo	21.2 - 32.2	9 - 31.7	Prog. Theor. Exp. Phys. 2015 (2015) 043D02
Sekihara, Oset, Ramos	16	72	Prog. Theor. Exp. Phys. 2016 (2016) 123D03
Phen. approach	BE [MeV]	Γ [MeV]	Reference
Akaishi, Yamazaki	48	61	Phys. Rev. C 65 (2002) 044005
Ikeda, Sato	60 - 95	45 - 90	Phys. Rev. C 76 (2007) 035203
Shevchenko, Gal, Mares	55 - 70	90 - 110	Phys. Rev. Lett. 98 (2007) 082301
Revai, Shevchenko	32	49	Phys. Rev. C 90 no. 3 (2014) 034004
Maeda, Akaishi, Yamazaki	51.5	61	Proc. Jpn. Acad. B 89 (2013) 418
Wycech, Green	40 - 80	40 - 85	Phys. Rev. C 79 (2009) 014001

Experiment	BE [MeV]	Γ [MeV]	Reference
FINUDA	$115_{-5}^{+6}(\text{stat.})_{-4}^{+3}(\text{sys.})$	$67_{-11}^{+14}(\text{stat.})_{-3}^{+2}(\text{sys.})$	PRL 94 (2005), 212303
OBELIX	160.9 ± 4.9	$< 24.4 \pm 8.0$	NPA 789 (2007), 222
E549	-	-	MPLA 23 (2008), 2520
DISTO	$103 \pm 3(\text{stat.}) \pm 5(\text{sys.})$	$118 \pm 8(\text{stat.}) \pm 10(\text{sys.})$	PRL 104 (2010), 132502
LEPS/SPring-8	Upper limit		PLB 728 (2014), 616
HADES	Upper limit		PLB 742 (2015), 242
E27	$95_{-17}^{+18}(\text{stat.})_{-21}^{+30}(\text{sys.})$	$162_{-45}^{+87}(\text{stat.})_{-78}^{+66}(\text{sys.})$	PTEP (2015), 021D01
AMADEUS	Upper limit		PLB 758 (2016), 134
E15 1st run	$15_{-8}^{+6}(\text{stat.}) \pm 12(\text{sys.})$	$110_{-17}^{+19}(\text{stat.}) \pm 27(\text{sys.})$	PTEP (2016), 051D01
E15 2nd run	$47 \pm 3(\text{stat.})_{-6}^{+3}(\text{sys.})$	$115 \pm 7(\text{stat.})_{-20}^{+10}(\text{sys.})$	PLB 789 (2019), 612

Possible existence of kaonic bound states



FINUDA, E549, E15, AMADEUS: K^{-} induced reactions
DISTO, HADES: p-p collisions
OBELIX: anti-p annihilations
E27: π induced reactions
LEPS/SPring-8: photoproduction

AMADEUS @ DAΦNE



DAΦNE

- $\phi \rightarrow K^- K^+$ (49.2%), $\approx 1000 \phi/s$
- monochromatic **low momentum**
Kaons $\approx 127 \text{ MeV}/c$
- **back to back** $K^- K^+$ topology
- **small hadronic background** due to the beam

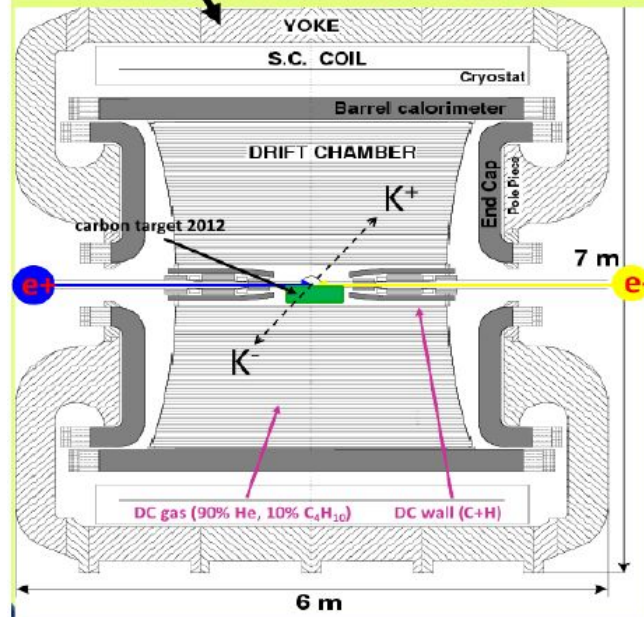
AMADEUS: KLOE 2004-2005 dataset analysis ($\mathcal{L} = 1.74 \text{ pb}^{-1}$)

Possibility to use **KLOE materials** as an **active target**

- DC wall (750 μm C foil, 150 μm Al foil);
- DC gas (90% He, 10% C_4H_{10}).

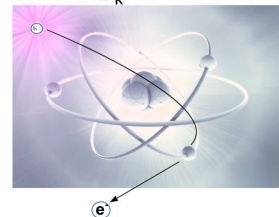
KLOE

- Cylindrical DC with **4π geometry** & electromagnetic calorimeter
- **96% acceptance**
- **high efficiency and resolution** for charged and neutral particles
- **exclusive measurement** of the considered



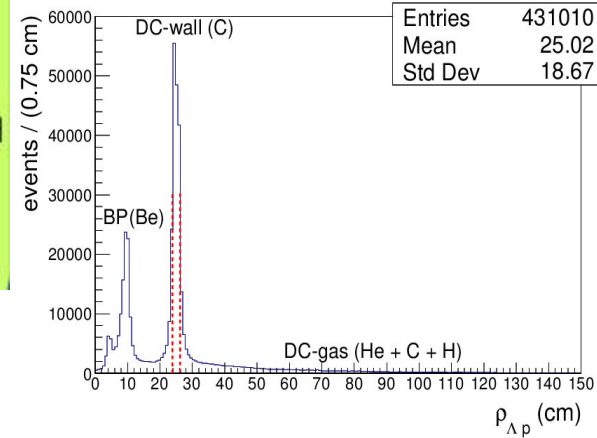
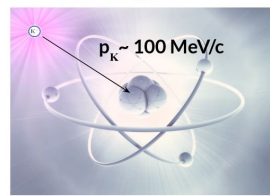
AT-REST

K^- absorbed from atomic orbitals
($p_K \sim 0 \text{ MeV}/c$)



IN-FLIGHT

($p_K \sim 100 \text{ MeV}/c$)



$\Lambda\pi^-$ analysis: K^-n non-resonant transition amplitude

$\Lambda(1405)$ case

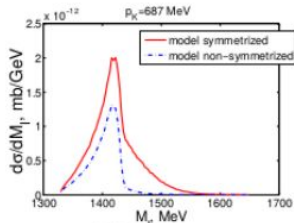


FIG. 4: Theoretical $(\pi^0\Sigma^0)$ invariant mass distribution for an initial kaon lab momenta of 687 MeV. The non-symmetrized distribution also contains the factor 1/2 in the cross section.

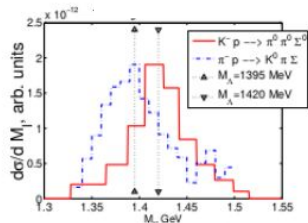
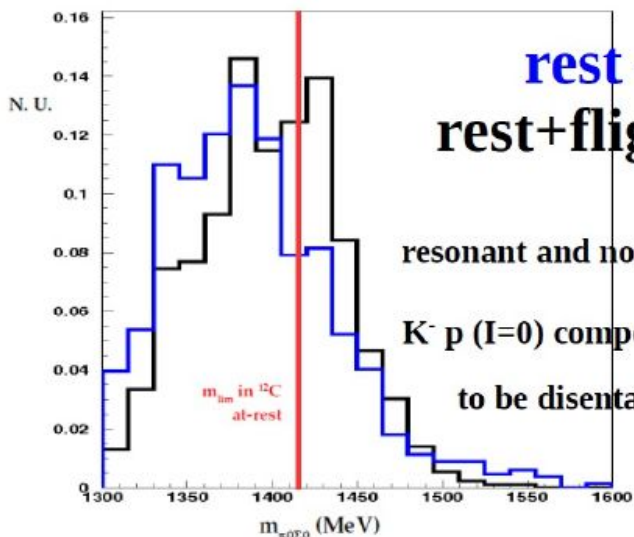


FIG. 5: Two experimental shapes of $\Lambda(1405)$ resonance. See text for more details.

IN FLIGHT $K^-^{12}C$ opens window between 1416 MeV and KN threshold

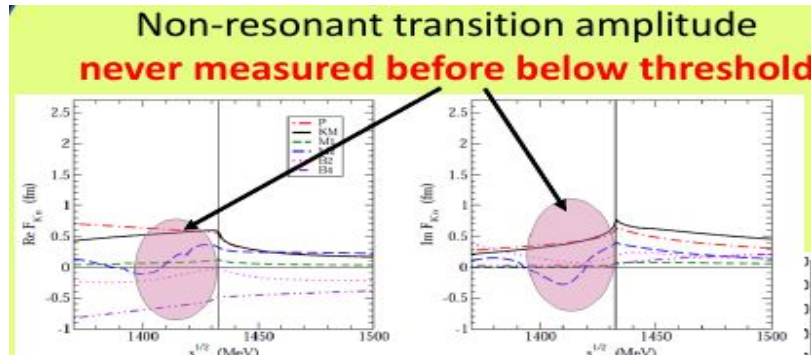


rest – rest+flight –

resonant and non-resonant

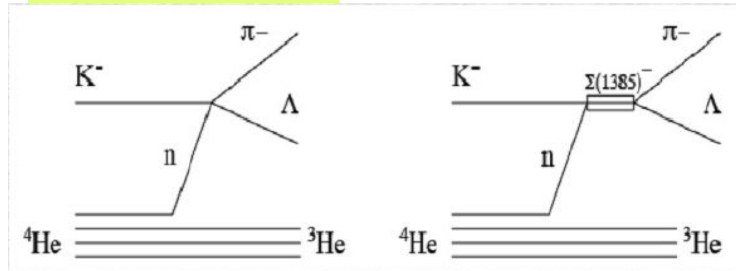
K^-p ($I=0$) components are to be disentangled

Goal: how much comes from resonance in $K^-N \rightarrow Y\pi$



J. Hrtankova, J. Mares, Phys. Rev. C96, 015205 (2017)
A. Cieply et al, Nucl. Phys. A 954, 17 (2016)

$K^-n \rightarrow \Lambda\pi^-$ direct formation in 4He

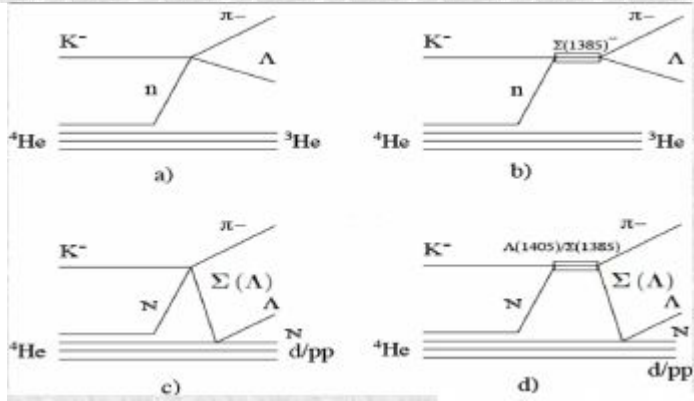


$$|f^{N-R}_{\Lambda\pi}(I=1)| \rightarrow |f^{N-R}_{\Sigma\pi}(I=0)|$$

K^- $^4\text{He} \rightarrow \Lambda p^-$ ^3He resonant and non-resonant processes

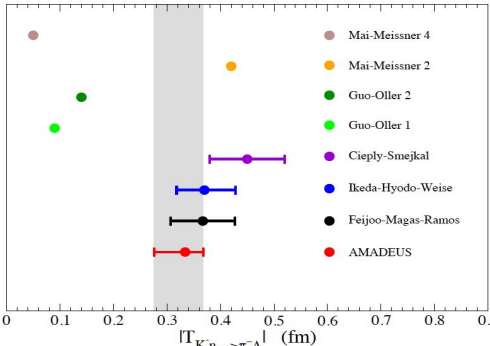
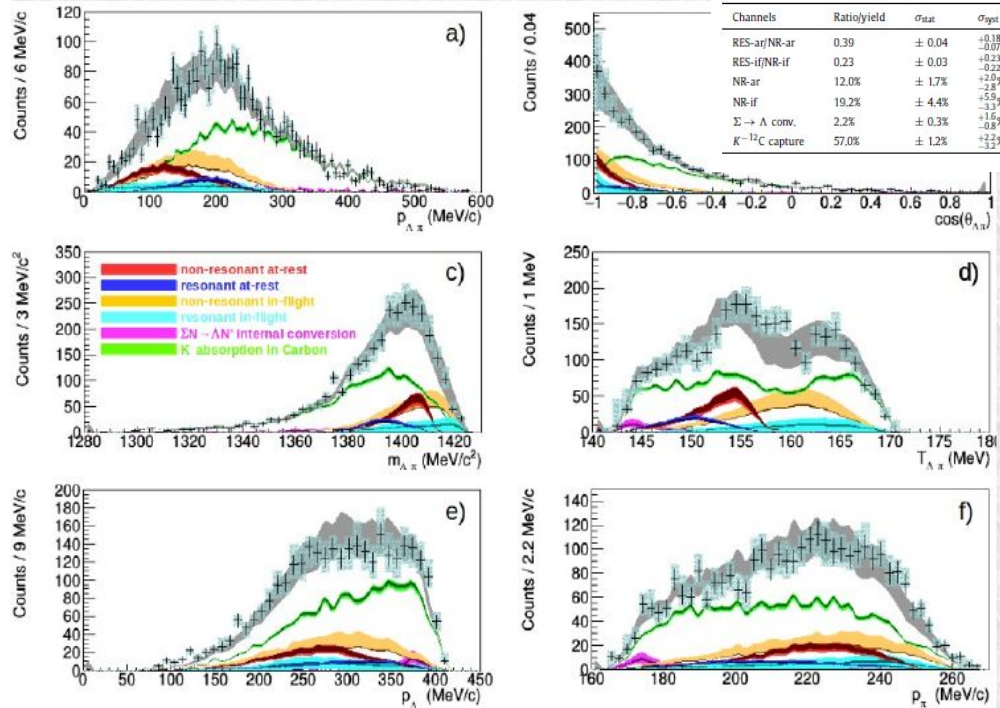
K. P., S. Wycech and C. Curceanu, Nucl. Phys. A954 (2016) 75-93

R. Del Grande, K. P., S. Wycech, Acta Phys. Pol. B 48 (2017) 1881



Simulations for resonant and non-resonant processes performed based on calculations for both S-state and P-state K-capture AT REST and IN FLIGHT

Simultaneous fit: $(p_{\Lambda\pi^-} - m_{\Lambda\pi^-} - \cos(\theta_{\Lambda\pi^-}))$



From the well known Σ^* transition probability:

$$\frac{NR - ar}{RES - ar} = \frac{\int_0^{p_{max}} P_{ar}^{nr}(p_{\Lambda\pi}) dp_{\Lambda\pi}}{\int_0^{p_{max}} P_{res}^{res}(p_{\Lambda\pi}) dp_{\Lambda\pi}} = |f_{ar}^s|^2 \cdot 8,94 \cdot 10^5 \text{MeV}^2$$

$$|f_{ar}^{nr}| = |A_{K^- n \rightarrow \Lambda\pi^-}| = (0.334 \pm 0.018 \text{ stat}^{+0.034}_{-0.058} \text{ syst}) \text{ fm}$$

- extract the amplitude for each model .. $A_{K^- n} = (\text{Re}F_{K^- n}^2 + \text{Im}F_{K^- n}^2)^{1/2}$
- scale the amplitudes for the $K^- n$ couplings to the $\Sigma\pi^0$ and $\Sigma^0\pi^-$ channels:

$$\frac{Prob_{K^- n \rightarrow \Lambda\pi^-}}{Prob_{K^- n \rightarrow \Sigma^0\pi^-}} = \frac{Ph_{K^- n \rightarrow \Lambda\pi^-}}{c_1 Ph_{K^- n \rightarrow \Sigma^0\pi^-}}$$

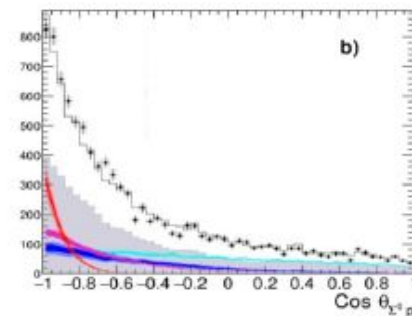
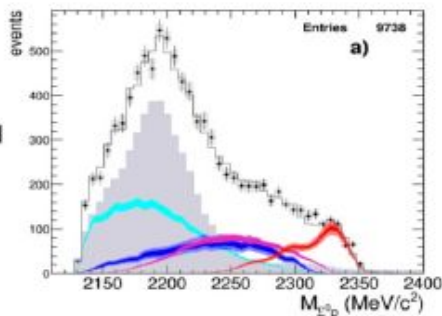
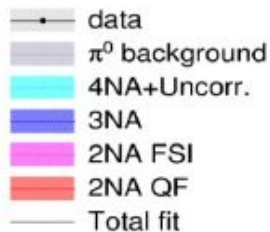
Isospin (1, 1) = (1, -1) component

$$\frac{Prob_{K^- n \rightarrow \Lambda\pi^-}}{Prob_{K^- n \rightarrow \Sigma^0\pi^-}} = \frac{Ph_{K^- n \rightarrow \Lambda\pi^-}}{c_2 Ph_{K^- n \rightarrow \Sigma^0\pi^-}}$$

Phase spaces ratios

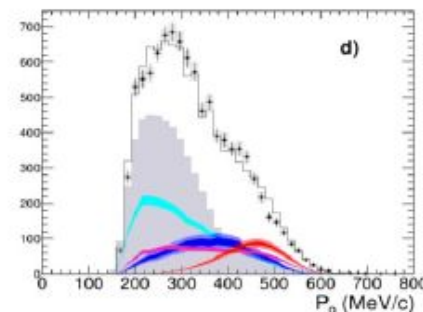
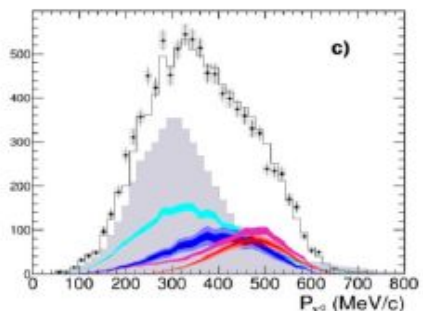
Σ^0 p analysis: K^- multi-nucleon absorptions in ^{12}C

Final fit

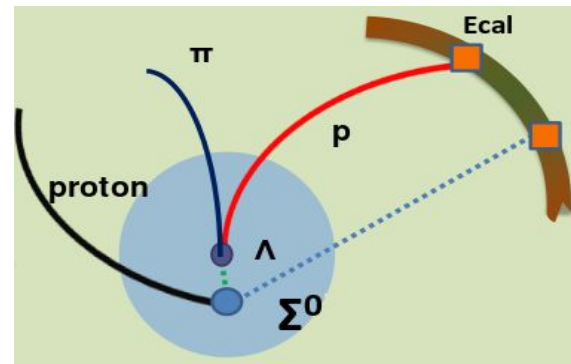


$$\chi^2 = 0.85$$

2NA-QF clearly separated from other processes



detected particles



No statistically significant bound state emerges at 2σ level

	yield / $K^-_{stop} \cdot 10^{-2}$	$\sigma_{stat} \cdot 10^{-2}$	$\sigma_{syst} \cdot 10^{-2}$
2NA-QF	0.127	± 0.019	+0.004 -0.008
2NA-FSI	0.272	± 0.028	+0.022 -0.023
Tot 2NA	0.376	± 0.033	+0.023 -0.032
3NA	0.274	± 0.069	+0.044 -0.021
Tot 3body	0.546	± 0.074	+0.048 -0.033
4NA + bkg.	0.773	± 0.053	+0.025 -0.076

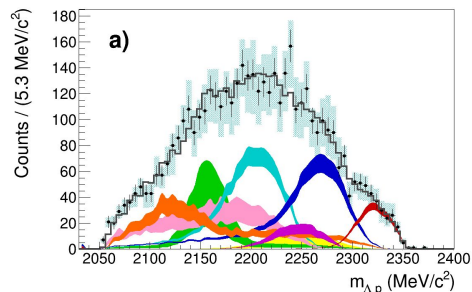
O. Vazquez Doce, et. al., Phys. Lett. B758, 134 (2016)

Λp analysis: K^- multi-nucleon absorption BRs and σ

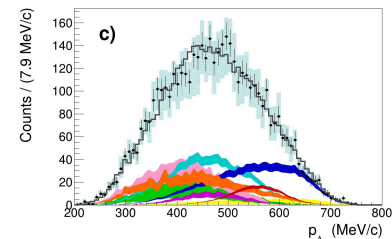
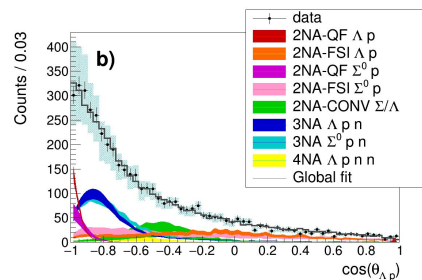
Simultaneous fit of:

- Λp invariant mass;
- angular correlation;
- proton momentum;
- Λ momentum.

Total reduced χ^2 : $\chi^2/dof = 0.94$



R. Del Grande et al., Eur.Phys.J. C79 (2019) no.3, 190

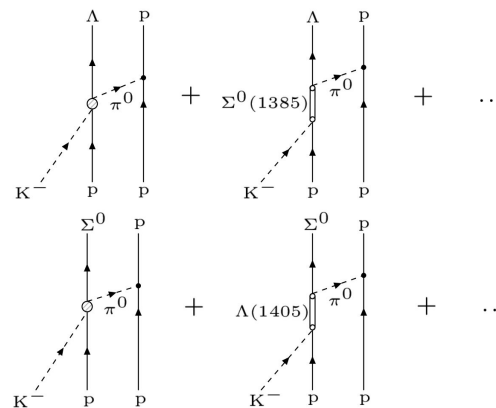


Process	Branching Ratio (%)	σ (mb)	@	p_K (MeV/c)
2NA-QF Λp	0.25 ± 0.02 (stat.) $^{+0.01}_{-0.02}$ (syst.)	2.8 ± 0.3 (stat.) $^{+0.1}_{-0.2}$ (syst.)	@	128 ± 29
2NA-FSI Λp	6.2 ± 1.4 (stat.) $^{+0.5}_{-0.6}$ (syst.)	69 ± 15 (stat.) ± 6 (syst.)	@	128 ± 29
2NA-QF $\Sigma^0 p$	0.35 ± 0.09 (stat.) $^{+0.13}_{-0.06}$ (syst.)	3.9 ± 1.0 (stat.) $^{+1.4}_{-0.7}$ (syst.)	@	128 ± 29
2NA-FSI $\Sigma^0 p$	7.2 ± 2.2 (stat.) $^{+4.2}_{-5.4}$ (syst.)	80 ± 25 (stat.) $^{+46}_{-60}$ (syst.)	@	128 ± 29
2NA-CONV Σ/Λ	2.1 ± 1.2 (stat.) $^{+0.9}_{-0.5}$ (syst.)	-	-	-
3NA $\Lambda p n$	1.4 ± 0.2 (stat.) $^{+0.1}_{-0.2}$ (syst.)	15 ± 2 (stat.) ± 2 (syst.)	@	117 ± 23
3NA $\Sigma^0 p n$	3.7 ± 0.4 (stat.) $^{+0.2}_{-0.4}$ (syst.)	41 ± 4 (stat.) $^{+2}_{-5}$ (syst.)	@	117 ± 23
4NA $\Lambda p n n$	0.13 ± 0.09 (stat.) $^{+0.08}_{-0.07}$ (syst.)	-	-	-
Global $\Lambda(\Sigma^0)p$	21 ± 3 (stat.) $^{+5}_{-6}$ (syst.)	-	-	-

The ratio between the branching ratios of the 2NA-QF in the Λp channel and in the $\Sigma^0 p$ is measured to be:

$$\mathcal{R} = \frac{BR(K^- pp \rightarrow \Lambda p)}{BR(K^- pp \rightarrow \Sigma^0 p)} = 0.7 \pm 0.2(\text{stat.})^{+0.2}_{-0.3}(\text{syst.})$$

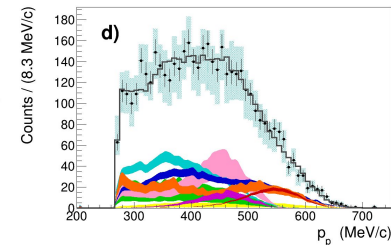
and the ratio between the corresponding phase spaces is $\mathcal{R}' \simeq 1.22$.



According to the pion exchange model:

$$\frac{BR(K^- pp \rightarrow \Lambda p)}{BR(K^- pp \rightarrow \Sigma^0 p)} = \frac{BR(K^- p \rightarrow \Lambda \pi^0)}{BR(K^- p \rightarrow \Sigma^0 \pi^0)}$$

[E. Oset and H. Toki, Phys. Rev. C 74 (2006) 015207]

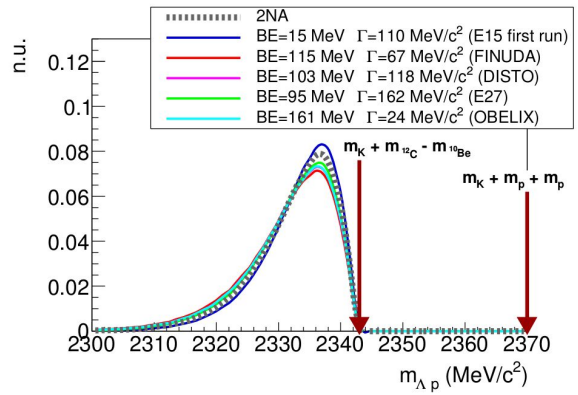


information on the in-medium properties of the Λ (1405).

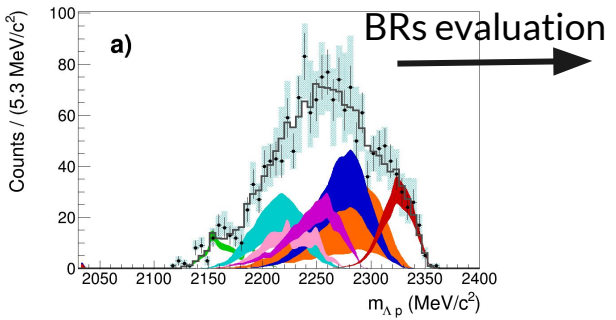
Λp analysis: $K^- pp$ bound state search

R. Del Grande et al., Eur.Phys.J. C79 (2019) no.3, 190

Using BE and Γ from experiments:

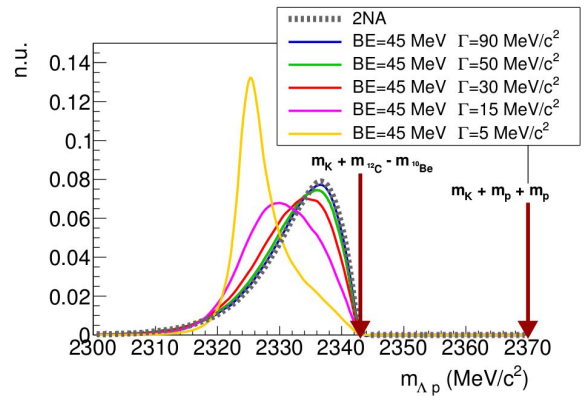


AMADEUS at DAΦNE

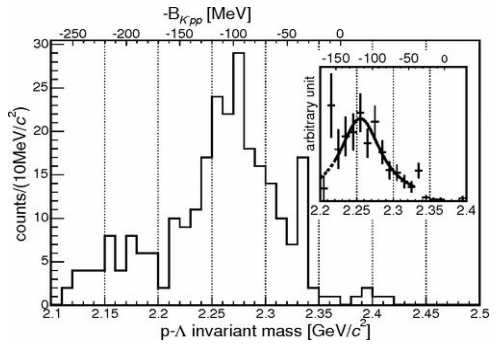


Process	Branching Ratio (%)
2NA-QF Λp	$0.20 \pm 0.04(\text{stat.}) \pm 0.02(\text{syst.})$
2NA-FSI Λp	$3.8 \pm 2.3(\text{stat.}) \pm 1.1(\text{syst.})$
2NA-QF $\Sigma^0 p$	$0.54 \pm 0.20(\text{stat.}) \begin{smallmatrix} +0.20 \\ -0.16 \end{smallmatrix}(\text{syst.})$
2NA-FSI $\Sigma^0 p$	$5.4 \pm 1.5(\text{stat.}) \begin{smallmatrix} +1.0 \\ -2.7 \end{smallmatrix}(\text{syst.})$
2NA-CONV Σ/Λ	$22 \pm 4(\text{stat.}) \begin{smallmatrix} +1 \\ -12 \end{smallmatrix}(\text{syst.})$
3NA Λpn	$1.1 \pm 0.3(\text{stat.}) \pm 0.2(\text{syst.})$
3NA $\Sigma^0 pn$	$1.9 \pm 0.7(\text{stat.}) \begin{smallmatrix} +0.8 \\ -0.4 \end{smallmatrix}(\text{syst.})$

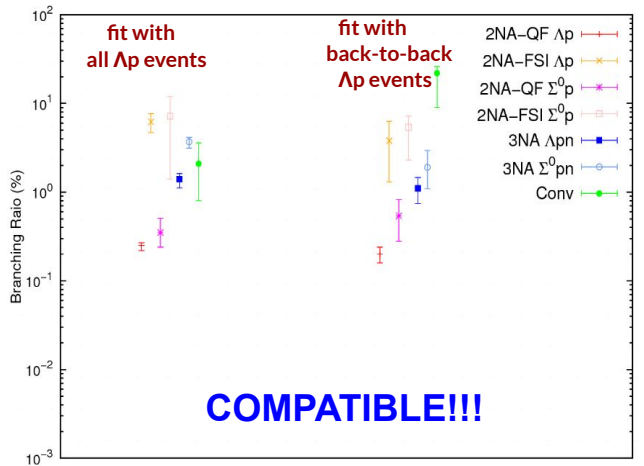
Fixing BE and moving Γ :



FINUDA at DAΦNE



[M. Agnello et al., Phys. Rev. Lett. 94, 212303 (2005)]



At analysis: Cross section and BR for 4NA in $K^- ^4\text{He} \rightarrow \text{At}$ process

Previous data:

- in ^4He : bubble chamber experiment

/M. Roosen, J. H. Wickens, II Nuovo Cimento 66, 101 (1981)/

only 3 events compatible with At kinematics found

$\text{BR}(K^- ^4\text{He} \rightarrow \text{At}) = (3 \pm 2) \times 10^{-4} / K_{\text{stop}}$ → global, no 4NA

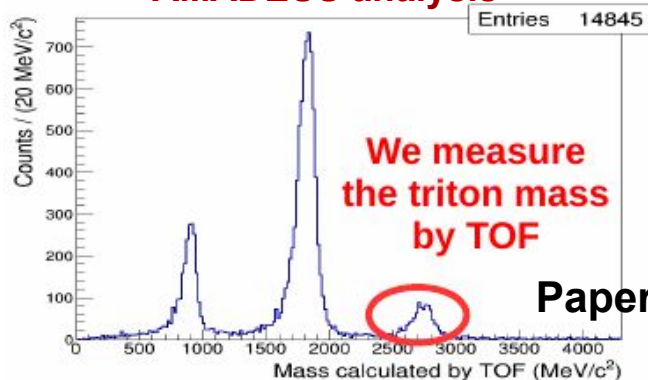
- in solid targets: $^6,7\text{Li}$, ^9Be (FINUDA)

/Phys. Lett. B, 229 (2008)/

40 events, only back-to-back data

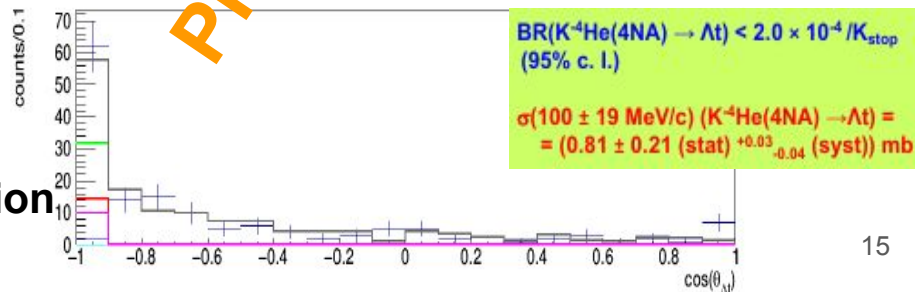
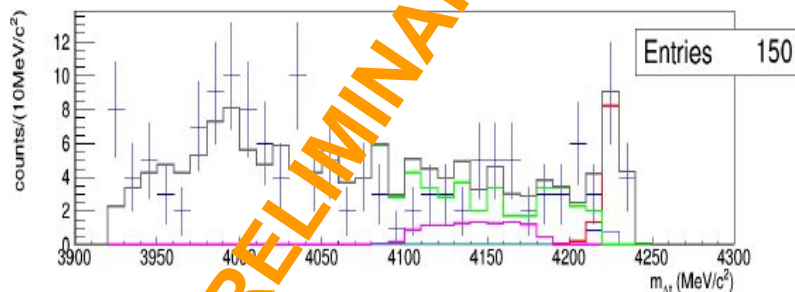
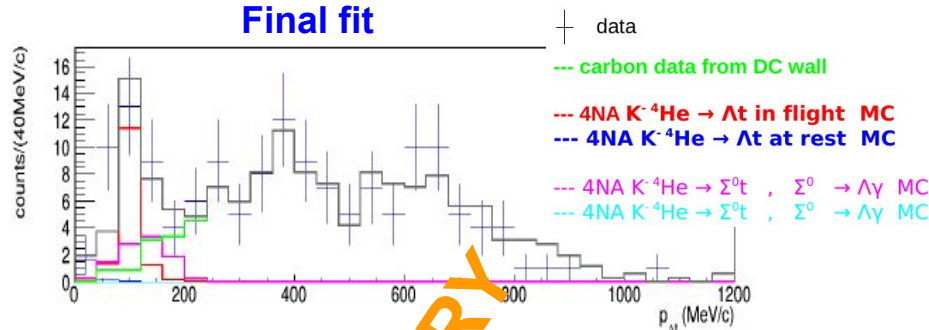
At emission yield → $10^{-3} - 10^{-4} / K_{\text{stop}}$ → global, no 4NA

AMADEUS analysis



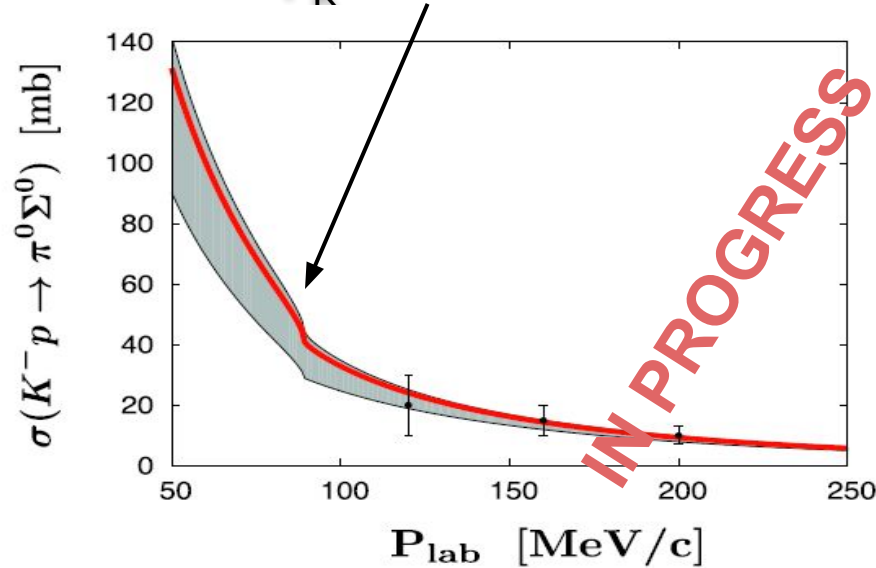
Paper in preparation

Final fit



$\Sigma^0\pi^0$ analysis

Goal: measurement of the $K^- p \rightarrow \Sigma^0\pi^0$ cross sections
for $p_K = 98 \pm 10$ MeV/c



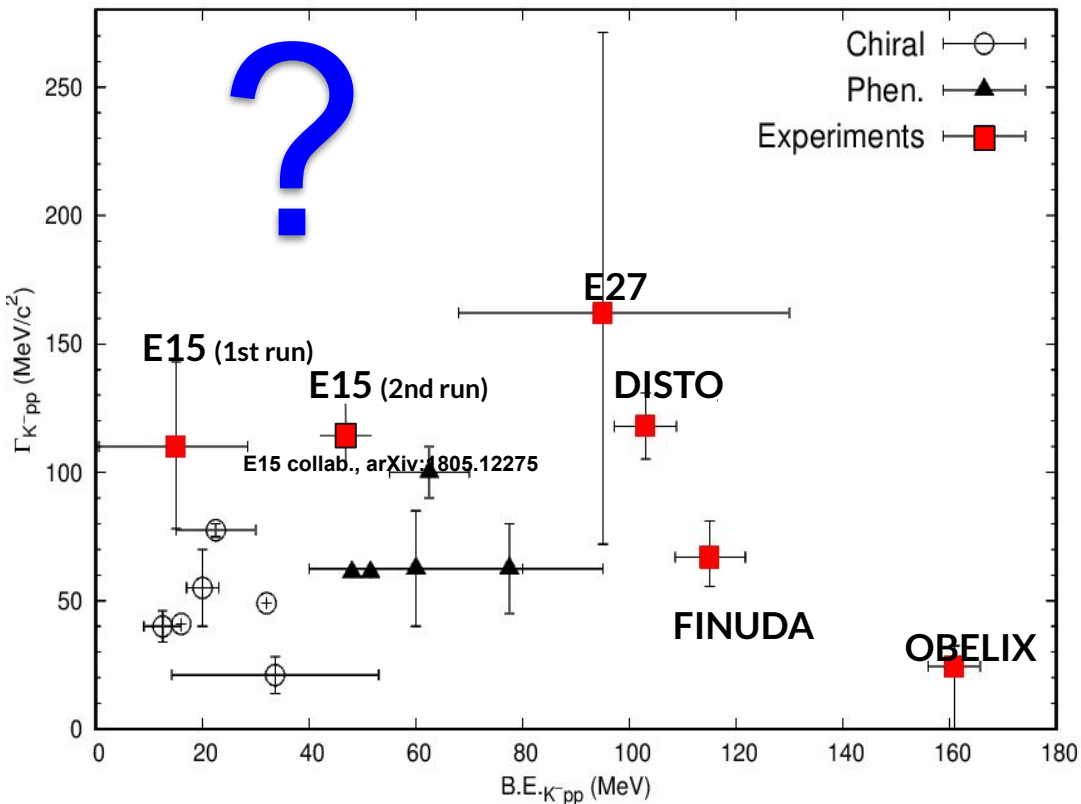
Y. Ikeda, T Hyodo, W. Weise, et. al., Phys. Lett. B706, 63 (2011); Nucl. Phys. A881, 98 (2012)

Low momentum K^- scattering cross sections in this Isospin $I = 0$ channel represent a fundamental input for the non-perturbative low energy QCD models



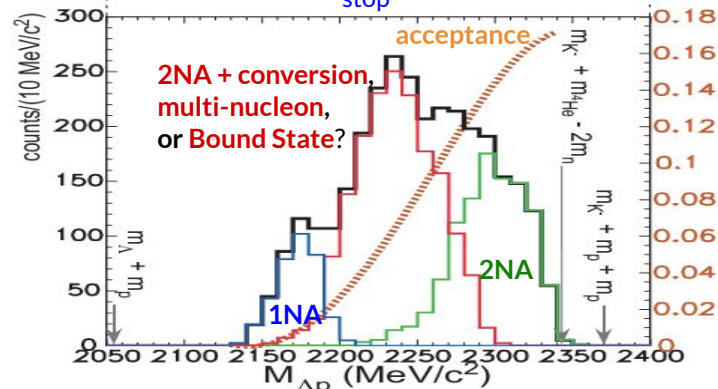
Thank you for attention!

How deep can be bound antikaon in nucleus?



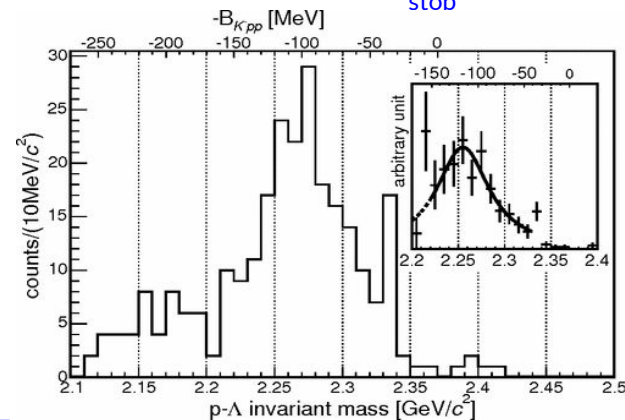
Experimental search in K^- induced reactions

E549 at KEK: $K^-_{\text{stop}} + {}^4\text{He} \rightarrow \Lambda + p + X'$



T. Suzuki et al., Mod. Phys. Lett. A23 (2008) 2520-2523

FINUDA at DAΦNE: $K^-_{\text{stop}} + X \rightarrow \Lambda + p + X'$



$BE = (115^{+3}_{-5} \text{ (stat.)}^{+3}_{-4} \text{ (syst.)}) \text{ MeV}$
 $\Gamma = (67^{+14}_{-11} \text{ (stat.)}^{+2}_{-3} \text{ (syst.)}) \text{ eV}/c^2$

AMADEUS @ DAΦNE

KLOE-at-DAΦNE
Laboratori Nazionali di Frascati



DAΦNE

- $\phi \rightarrow K^- K^+$ (49.2%), $\approx 1000 \phi/s$
- monochromatic **low momentum**
Kaons $\approx 127 \text{ MeV}/c$
- **back to back** $K^- K^+$ topology
- **small hadronic background** due to the beam

AMADEUS: KLOE 2004-2005 dataset analysis ($\mathcal{L} = 1.74 \text{ pb}^{-1}$)

AMADEUS scientific case

- nature of $\Lambda(1405)$ and K^-N amplitude below threshold

- K^- multiN absorption

- kaonic nuclear clusters



YN correlation studies
($\Lambda p, \Sigma^0 p, \Lambda t$)

- low-energy charged K cross section (for $p=100 \text{ MeV}$)

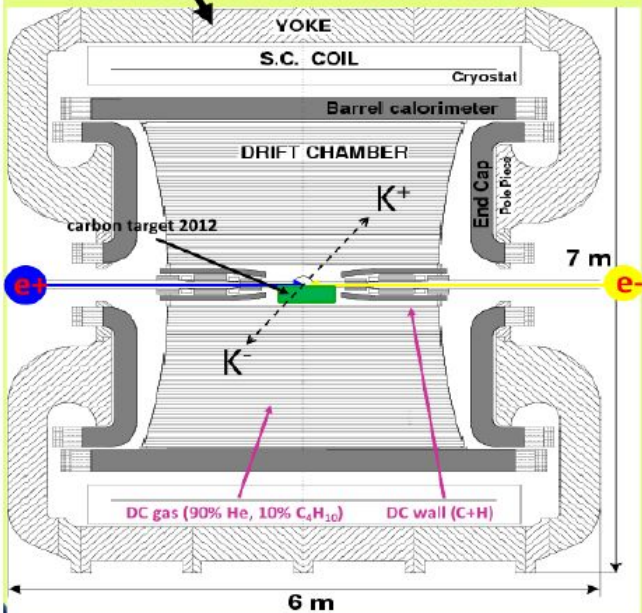
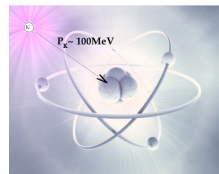
KLOE

- Cylindrical DC with 4π geometry & electromagnetic calorimeter
- **96% acceptance**
- **high efficiency and resolution** for charged and neutral particles
- exclusive measurement of the considered

**K^- absorption on light nuclei
AT REST & IN FLIGHT**

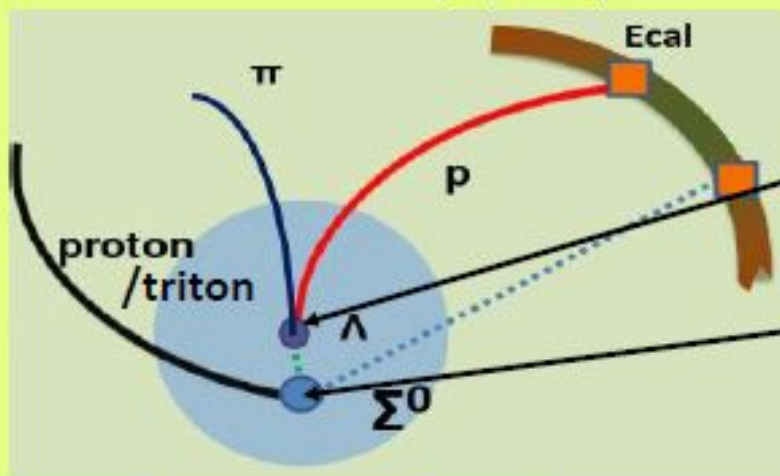


K^- absorbed from atomic orbit



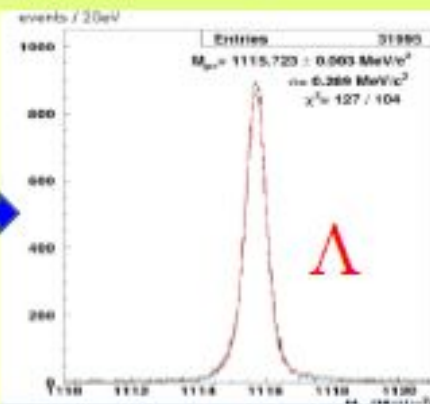
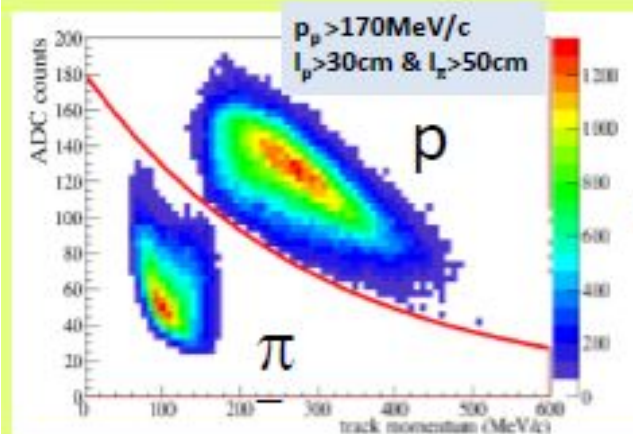
$K^- ^{12}\text{C} \rightarrow \Lambda/\Sigma^0 \text{ p (2NA)}$

$K^- ^4\text{He} \rightarrow \Lambda/\Sigma^0 \text{ t (4NA)}$

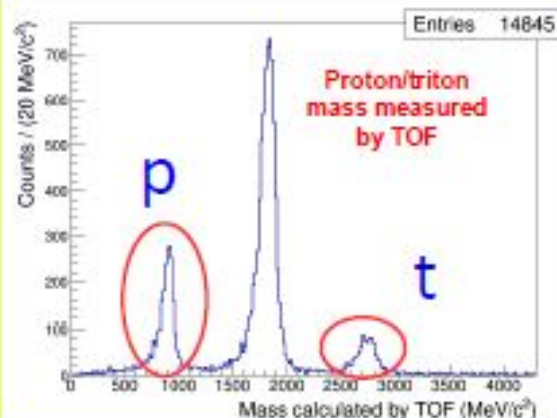


Λ decay vertex

hadronic vertex

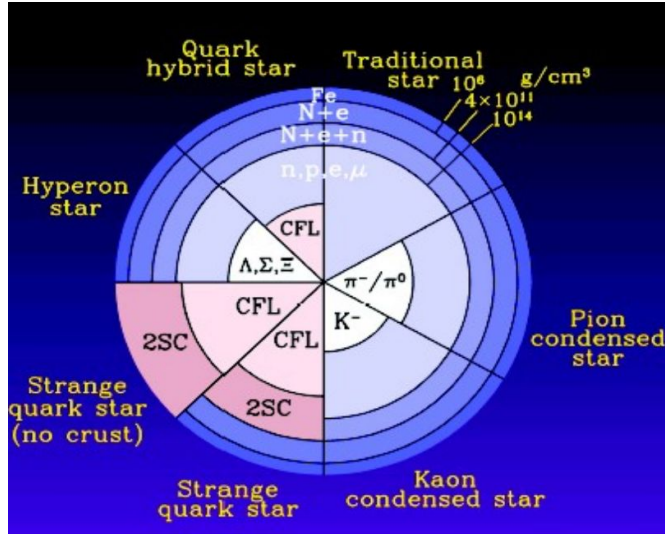


$1112 < M_{p\pi} < 1118 \text{ MeV}/c^2$

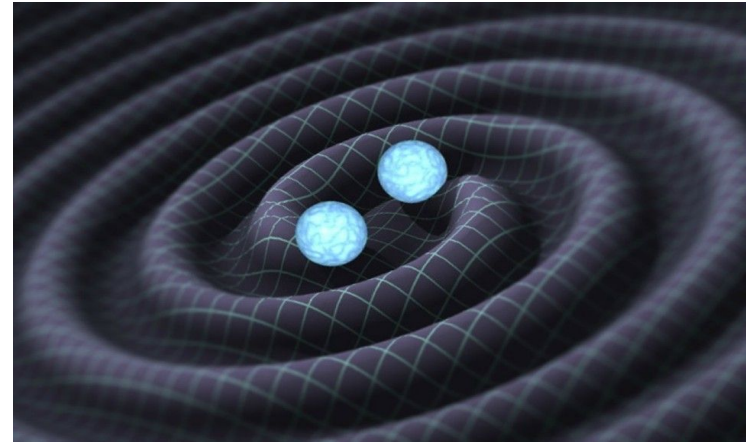
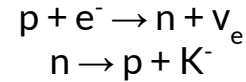


Essential impact on the EoS of Neutron Stars

Role of strangeness in dense baryonic matter, kaon condensation? Strange quark matter? Hyperons in Neutron Stars?



The central densities are expected to be large enough to activate the strangeness production:



HOT TOPIC after the measurement of the gravitational waves signal emitted by binary system of Neutron Stars (GW170817)

YN/NN scatterings

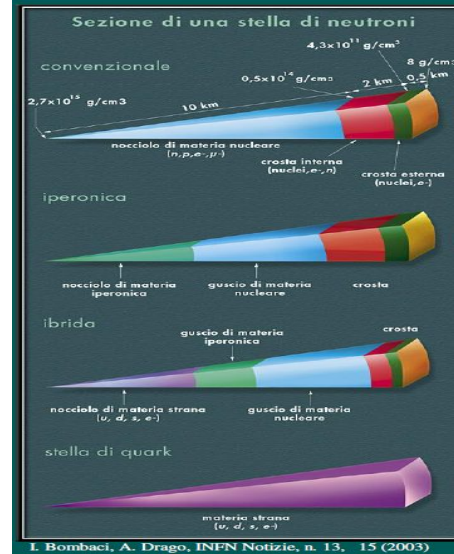
Y-N/NN interaction essential impact on the case of NEUTRON STARS

ECT*, Trento (Italy), 27 – 31 October 2014

Strangeness in Neutron Stars

Ignazio Bombaci

Dipartimento di Fisica “E. Fermi”, Università di Pisa
INFN Sezione di Pisa



“Neutron

Nucleon Stars

Hyperon Stars

Hybrid Stars

Strange Stars

Microscopic approach to hyperonic matter EOS

input

2BF: nucleon-nucleon (NN), nucleon-hyperon (NY), hyperon-hyperon (YY)

e.g. Nijmegen, Julich models

3BF: NNN, NNY, NYY, YYY

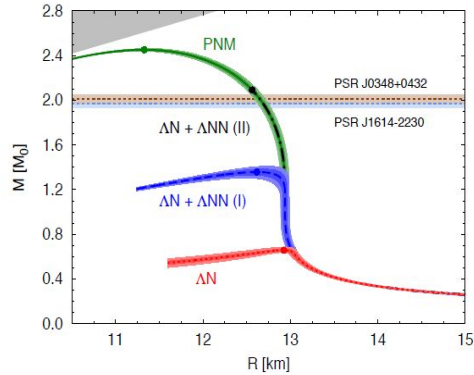
Hyperonic sector: experimental data

- 1. YN scattering** (very few data)
- 2. Hypernuclei**

YN/NN scatterings

No experimental information on Σ^0 -N/NN interaction

Λ -neutron matter



Lonardonì, Lovato, Gandolfi, Pederiva, PRL (2015)

Drastic role played by Λ NN. Calculations can be compatible with neutron star observations.

Note: no ν_{Λ} , no protons, and no other hyperons included yet...

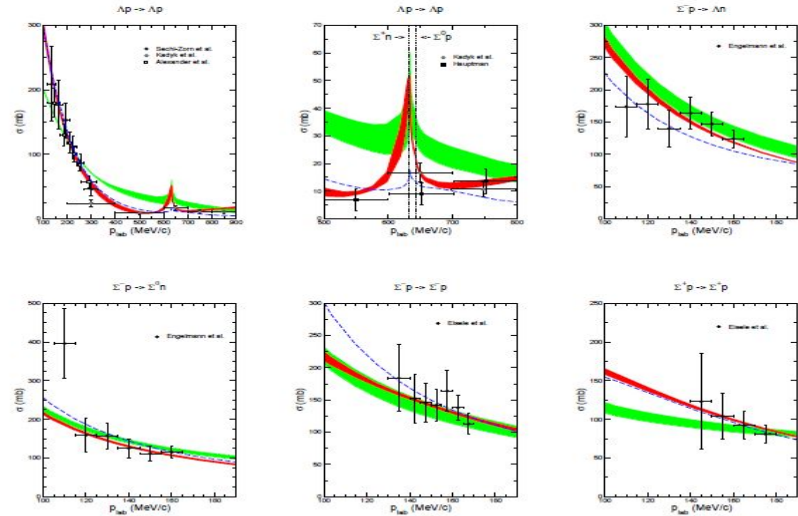


Figure 2: "Total" cross section σ (as defined in Eq. (24)) as a function of p_{lab} . The experimental cross sections are taken from Refs. [52] (filled circles), [53] (open squares), [65] (open circles), and [66] (filled squares) ($\Lambda p \rightarrow \Lambda p$), from [54] ($\Sigma^- p \rightarrow \Lambda n$, $\Sigma^- p \rightarrow \Sigma^0 n$) and from [55] ($\Sigma^- p \rightarrow \Sigma^- p$, $\Sigma^+ p \rightarrow \Sigma^+ p$). The red/dark band shows the chiral EFT results to NLO for variations of the cutoff in the range $\Lambda = 500, \dots, 650$ MeV, while the green/light band are results to LO for $\Lambda = 550, \dots, 700$ MeV. The dashed curve is the result of the Jülich '04 meson-exchange potential [36].

Nucl. Phys. A 915 (2013) 24-58